Jun Dong
Graduate Research Assistant
e-mail: jundong@ccad.uiowa.edu

Kyung K. Choi
Carver Professor
Fellow ASME
e-mail: kkchoi@ccad.uiowa.edu

Department of Mechanical and Industrial Engineering and
Center for Computer-Aided Design,
The University of Iowa, Iowa City, IA 52242

Nam H. Kim
Assistant Professor,
e-mail: nkim@ufl.edu
Department of Mechanical and Aerospace Engineering,
The University of Florida,
PO Box 116300, Gainesville, FL 32611-6300

Design Optimization for Structural-Acoustic Problems Using FEA-BEA With Adjoint Variable Method

A noise-vibration-harshness (NVH) design optimization of a complex vehicle structure is presented using finite element and boundary element analyses. The steady-state dynamic behavior of the vehicle is calculated from the frequency response finite element analysis, while the sound pressure level within the acoustic cavity is calculated from the boundary element analysis. A reverse solution process is employed for the design sensitivity calculation using the adjoint variable method. The adjoint load is obtained from the acoustic boundary element re-analysis, while the adjoint solution is calculated from the structural dynamic re-analysis. The evaluation of pressure sensitivity only involves a numerical integration process over the structural part where the design variable is defined. A design optimization problem is formulated and solved, where the structural weight is reduced while the noise level in the passenger compartment is lowered.
[DOI: 10.1115/1.1701879]

1 Introduction

The design of a vehicle with high ride quality draws attention of engineers increasingly due to the customer's preference. Especially, the structural-acoustic performance of a passenger vehicle becomes an important issue in the design process. The purpose of this paper is to show feasibility of design optimization to minimize the vehicle's weight subjected to the structural-acoustic constraints. Many numerical methods have been developed to simulate the structural-acoustic performance of a passenger vehicle. The finite element method [1], the boundary element method [2], the statistical energy analysis [3,4], and the energy flow analysis [5–7] are a short list of methods that can be used for the purpose. Different methods must be used based on the design interest. For example, the finite element analysis (FEA) and boundary element analysis (BEA) can be used for simulation in the low-frequency range, while the statistical energy analysis and energy flow analysis can be used for the high-frequency range. In this paper, the former methods are employed to simulate the vehicle's structural-acoustic performance in the 1–100 Hz frequency range. A commercial finite element code MSC/NASTRAN [8] is used to simulate the frequency response of the vehicle structure, while a boundary element code COMET/ACOUSTICS [9] is used to calculate the sound pressure level in the cabin compartment based on the velocity information obtained from the finite element code. That is, the simulation procedure is sequential and uncoupled based on the assumption that the vibration of the air does not contribute to the structural vibration.

Many research results [10–18] have been published in design sensitivity analysis (DSA) of structural-acoustic problems using FEA and BEA. While the direct differentiation method in DSA follows the same solution process as the response analysis, the adjoint variable method follows a reverse process. One of the challenges of the adjoint variable method in sequential acoustic analysis is how to formulate this reverse process. The sequential adjoint variable method with a reverse solution process developed by Kim et al. [19,20] is used, in which the adjoint load is obtained from boundary element re-analysis, and the adjoint variable is calculated from structural dynamic reanalysis.

For NVH design optimization, design parameterization, design sensitivity analysis, and design optimization algorithms need to be integrated. The Design Sensitivity Analysis and Optimization (DSO) Tool [21] developed at the Center for Computer-Aided Design at the University of Iowa is used as an integrating environment in this paper. The graphic user interface in DSO allows the design engineers to carry out design parameterization, structural-acoustic analysis, design sensitivity analysis, and design optimization.

The proposed sequential structural-acoustic analysis and DSA using the adjoint variable method are applied to the optimization of a next generation concept vehicle model, by which the vehicle weight is minimized while the sound pressure level is constrained. A design optimization problem is formulated and solved, where the structural weight is reduced while the noise level in the passenger compartment is lowered.

2 Structural-Acoustic Analysis

2.1 Frequency Response Analysis. The steady-state response of a structure under the harmonic load $\mathbf{f}(\mathbf{x})$ with frequency ω can be written as

$$-\omega^2\rho\mathbf{z}(\mathbf{x})+j\omega C\mathbf{z}(\mathbf{x})+L\mathbf{z}(\mathbf{x})=\mathbf{f}(\mathbf{x}),\quad \mathbf{x}\in\Omega^S \tag{1}$$

where Ω^S is the structural domain, $\mathbf{z}(\mathbf{x})$ is the complex displacement, L is the linear partial differential operator, $\rho(\mathbf{x})$ is the mass density, and C is the viscous damping effect.

For the variational formulation, since the complex variable $\mathbf{z}(\mathbf{x})$ is used for the state variable, the complex conjugate $\overline{\mathbf{z}}^*$ is used for the variation of the state variable. By multiplying Eq. (1) with $\overline{\mathbf{z}}^*$ and integrating it over the structural domain Ω^S, the variational equation can be derived after integration by parts for the differential operator L as

Contributed by the Design Automation Committee for publication in the JOURNAL OF MECHANICAL DESIGN. Manuscript received October 2002; revised October 2003. Associate Editor: G. M. Fadel.

$$\int \int_{\Omega^S} [-\omega^2 \rho \mathbf{z}^T + j\omega C \mathbf{z}^T] \overline{\mathbf{z}}^* d\Omega^S + \int \int_{\Omega^S} \boldsymbol{\sigma}(\mathbf{z})^T \boldsymbol{\varepsilon}(\overline{\mathbf{z}}^*) d\Omega^S = \int \int_{\Omega^S} \mathbf{f}^{bT} \overline{\mathbf{z}}^* d\Omega^S + \int_{\Gamma^s} \mathbf{f}^{sT} \overline{\mathbf{z}}^* d\Gamma, \quad \forall \overline{\mathbf{z}} \in Z \tag{2}$$

where $\overline{\mathbf{z}}^*$ is the complex conjugate of the kinematically admissible virtual displacement $\overline{\mathbf{z}}$, and Z is the complex space of kinematically admissible virtual displacements. Equation (2) provides the variational equation of the dynamic frequency response under an oscillating excitation with frequency ω. For simplification of notation, the following terms are defined:

$$d_u(\mathbf{z}, \overline{\mathbf{z}}) = \int \int_{\Omega^S} \rho \mathbf{z}^T \overline{\mathbf{z}}^* d\Omega^S \tag{3}$$

$$c_u(\mathbf{z}, \overline{\mathbf{z}}) = \int \int_{\Omega^S} C \mathbf{z}^T \overline{\mathbf{z}}^* d\Omega^S \tag{4}$$

$$a_u(\mathbf{z}, \overline{\mathbf{z}}) = \int \int_{\Omega^S} \boldsymbol{\sigma}(\mathbf{z})^T \boldsymbol{\varepsilon}(\overline{\mathbf{z}}^*) d\Omega^S \tag{5}$$

$$\ell_u(\overline{\mathbf{z}}) = \int \int_{\Omega^S} \mathbf{f}^{bT} \overline{\mathbf{z}}^* d\Omega^S + \int_{\Gamma^s} \mathbf{f}^{sT} \overline{\mathbf{z}}^* d\Gamma \tag{6}$$

where $d_u(\cdot,\cdot)$ is the sesqui-linear kinetic energy form, $c_u(\cdot,\cdot)$ is the sesqui-linear damping form; $a_u(\cdot,\cdot)$ is the sesqui-linear strain energy form, and $\ell_u(\cdot)$ is the semi-linear load form. The definitions of the sesqui-linear and semi-linear forms can be found in Horvath [23].

Since the structure-induced pressure within the acoustic domain is related to the velocity of the structural response, it is convenient to transfer the displacement to the velocity using the following relation:

$$\mathbf{v}(\mathbf{x}) = j\omega \mathbf{z}(\mathbf{x}) \tag{7}$$

By using Eqs. (2)–(7), the variational equation of the frequency response problem can be obtained as

$$j\omega d_{\mathbf{u}}(\mathbf{v}, \overline{\mathbf{z}}) + c_{\mathbf{u}}(\mathbf{v}, \overline{\mathbf{z}}) + \frac{1}{j\omega} a_{\mathbf{u}}(\mathbf{v}, \overline{\mathbf{z}}) = \ell_{\mathbf{u}}(\overline{\mathbf{z}}), \quad \forall \overline{\mathbf{z}} \in Z \tag{8}$$

The structural damping, a variant of the viscous damping, is caused either by internal material friction or by connections among structural components. It has been experimentally observed that for each cycle of vibration, the dissipated energy of the material is proportional to the displacement [24]. When the damping coefficient is small as in the case of structures, damping is primarily effective at those frequencies close to the resonance. The variational equation with the structural damping effect is

$$j\omega d_u(\mathbf{v}, \overline{\mathbf{z}}) + \kappa a_u(\mathbf{v}, \overline{\mathbf{z}}) = \ell_u(\overline{\mathbf{z}}), \quad \forall \overline{\mathbf{z}} \in Z \tag{9}$$

where $\kappa = (1 + j\phi)/j\omega$ and ϕ is the structural damping coefficient. After the structure is discretized using finite elements, and kinematic boundary conditions are applied, the following system of matrix equations is obtained:

$$[j\omega \mathbf{M} + \kappa \mathbf{K}]\{\mathbf{v}(\omega)\} = \{\mathbf{f}(\omega)\} \tag{10}$$

where $[\mathbf{M}]$ is the mass matrix and $[\mathbf{K}]$ is the stiffness matrix.

2.2 Acoustic Boundary Element Analysis. Together with the structural velocity results, BEA is used to evaluate pressure response in the acoustic domain. In simplified notation, the boundary integral equation of the acoustic problem can be written as

$$b(\mathbf{x}_0; \mathbf{v}) + e(\mathbf{x}_0; p_S) = \alpha p(\mathbf{x}_0) \tag{11}$$

where $b(\mathbf{x}_0;\cdot)$ and $e(\mathbf{x}_0;\cdot)$ are linear integral forms that correspond to contributions from the surface velocity and surface pressure respectively. The constant α is equal to 1 for $\mathbf{x}_0$ inside the acoustic volume, 0.5 for $\mathbf{x}_0$ on a smooth boundary surface, and 0 for $\mathbf{x}_0$ outside the acoustic volume. Note that Eq. (11) can provide a solution for both radiation and interior acoustic problems. Unlike the energy forms in Eqs. (3)–(6), these integral forms are independent of the structural sizing design variable; thus no subscription $\mathbf{u}$ is used in their definitions.

The BEA is done in two steps: first evaluating the pressure on the acoustic boundary using the structural velocity, and then calculating the pressure within the acoustic domain using the boundary pressure information. Suppose the acoustic boundary S is approximated by N number of nodes. If observation point $\mathbf{x}_0$ is located at every boundary node, then the following linear system of equations is obtained from Eq. (11):

$$[\mathbf{A}]\{\mathbf{p}_S\} = [\mathbf{B}]\{\mathbf{v}\} \tag{12}$$

where $\{\mathbf{p}_S\} = \{p_1, p_2, \ldots, p_N\}^T$ is the nodal pressure vector, $\{\mathbf{v}\}$ is the $3N \times 1$ velocity vector, $[\mathbf{A}]$ is the $N \times N$ coefficient matrix, and $[\mathbf{B}]$ is the $N \times 3N$ coefficient matrix. Note that these vectors and matrices are all complex variables. The process of computing the boundary pressure $\{\mathbf{p}_S\}$ assumes domain discretization, and the condition in Eq. (11) is imposed in every node. However, for the purpose of DSA, let us consider a continuous counterpart to Eq. (12), defined as

$$A(\mathbf{p}_S) = B(\mathbf{v}) \tag{13}$$

where the integral forms $A(\cdot)$ and $B(\cdot)$ correspond to the matrices $[\mathbf{A}]$ and $[\mathbf{B}]$ in Eq. (12), respectively. The boundary pressure can then be calculated from $\mathbf{p}_S = A^{-1} \circ B(\mathbf{v})$. Once $\{\mathbf{p}_S\}$ has been computed, Eq. (11) can be used to compute the acoustic pressure at any point $\mathbf{x}_0$ within the acoustic domain in the form of a vector equation as

$$p(\mathbf{x}_0) = \{\mathbf{b}(\mathbf{x}_0)\}^T \{\mathbf{v}\} + \{\mathbf{e}(\mathbf{x}_0)\}^T \{\mathbf{p}_S\} \tag{14}$$

where $\{\mathbf{b}(\mathbf{x}_0)\}$ and $\{\mathbf{e}(\mathbf{x}_0)\}$ are the column vectors that correspond to the left-hand side of the boundary integral Eq. (11).

In the sizing design problem, in which panel thickness is a design variable, integral forms $b(\mathbf{x}_0;\cdot)$ and $e(\mathbf{x}_0;\cdot)$ in Eq. (11) are independent of the design variable. Only implicit dependence on the design exists through the state variables $\mathbf{v}$ and $\mathbf{p}_S$, which will be developed in the following section. However, in the shape design problem, the acoustic domain changes according to the structural domain change, which is a design variable. Thus, integral forms $b(\mathbf{x}_0;\cdot)$ and $e(\mathbf{x}_0;\cdot)$ will depend on the design.

3 Design Sensitivity Analysis

The purpose of DSA is to compute the dependency of performance measures on the design. In this study, only sizing design, such as the thickness of a plate and the cross-sectional dimension of a beam, is considered.

3.1 Direct Differentiation Method. The direct differentiation method computes the variation of state variables by differentiating the state Eqs. (9) and (11) with respect to the design. Let us first consider the structural part, i.e., the frequency response analysis in Eq. (9). The forms that appear in Eq. (9) explicitly depend on the design, and their variations are defined as

$$d'_{\delta \mathbf{u}}(\mathbf{v}, \overline{\mathbf{z}}) \equiv \frac{d}{d\tau} [d_{\mathbf{u}+\tau\delta\mathbf{u}}(\tilde{\mathbf{v}}, \overline{\mathbf{z}})] \Big|_{\tau=0} \tag{15}$$

$$a'_{\delta \mathbf{u}}(\mathbf{v}, \overline{\mathbf{z}}) \equiv \frac{d}{d\tau} [a_{\mathbf{u}+\tau\delta\mathbf{u}}(\tilde{\mathbf{v}}, \overline{\mathbf{z}})] \Big|_{\tau=0} \tag{16}$$

$$\ell'_{\delta \mathbf{u}}(\overline{\mathbf{z}}) \equiv \frac{d}{d\tau} [\ell_{\mathbf{u}+\tau\delta\mathbf{u}}(\overline{\mathbf{z}})] \Big|_{\tau=0} \tag{17}$$

where $\tilde{\mathbf{v}}$ denotes the state variable $\mathbf{v}$ with the dependence on τ being suppressed, and $\overline{\mathbf{z}}$ and its complex conjugate are independent of the design. The detailed expressions of $d'_{\delta u}(\cdot,\cdot)$, $a'_{\delta u}(\cdot,\cdot)$, and $\ell'_{\delta u}(\cdot)$ can be found in Kim et al. [19].

Thus, by taking a variation of both sides of Eq. (9) with respect to the design, and by moving explicitly dependent terms on the design to the right side, the following sensitivity equation can be obtained:

$$j\omega d_{\mathbf{u}}(\mathbf{v}',\overline{\mathbf{z}})+\kappa a_{\mathbf{u}}(\mathbf{v}',\overline{\mathbf{z}})=\ell'_{\delta\mathbf{u}}(\overline{\mathbf{z}})-j\omega d'_{\delta\mathbf{u}}(\mathbf{v},\overline{\mathbf{z}})-\kappa a'_{\delta\mathbf{u}}(\mathbf{v},\overline{\mathbf{z}}),\quad \forall\,\overline{\mathbf{z}}\in Z \tag{18}$$

Presuming that the velocity $\mathbf{v}$ is given as a solution to Eq. (9), Eq. (18) is a variational equation, with the same sesqui-linear forms for displacement variation $\mathbf{v}'$. Note that the stiffness matrices corresponding to Eqs. (9) and (18) are the same, and that the right side of Eq. (18) can be considered a fictitious load term. If a design perturbation $\delta\mathbf{u}$ is defined, and if the right side of Eq. (18) is evaluated with the solution of Eq. (9), then Eq. (18) can be numerically solved to obtain $\mathbf{v}'$ using FEA. By interpreting the right side of Eq. (18) as another load form, Eq. (18) can be solved by using the same solution process as the frequency response problem in Eq. (9).

Next the acoustic aspect will be considered, which is represented by the boundary integral Eq. (11). A direct differentiation of Eq. (11) yields the following sensitivity equation:

$$b(\mathbf{x}_0;\mathbf{v}')+e(\mathbf{x}_0;p'_S)=\alpha p'(\mathbf{x}_0) \tag{19}$$

Since integral forms $b(\mathbf{x}_0;\cdot)$ and $e(\mathbf{x}_0;\cdot)$ are independent of the design, the above equation has exactly the same form as Eq. (11). Thus, using the solution $\mathbf{v}'$ from the structural sensitivity Eq. (18), Eq. (19) can be solved by following the same solution process as BEA, to obtain the pressure sensitivity result. Thus, like Eq. (12), the following matrix equation has to be solved in the discrete system:

$$[\mathbf{A}]\{\mathbf{p}'_S\}=[\mathbf{B}]\{\mathbf{v}'\} \tag{20}$$

And then, like Eq. (14), the pressure sensitivity at point $\mathbf{x}_0$ can be obtained from

$$p'(\mathbf{x}_0)=\{\mathbf{b}(\mathbf{x}_0)\}^T\{\mathbf{v}'\}+\{\mathbf{e}(\mathbf{x}_0)\}^T\{\mathbf{p}'_S\} \tag{21}$$

This sensitivity calculation process is the same as the BEA solution process described from Eq. (12) to Eq. (14).

Consider a performance measure that is defined at point $\mathbf{x}_0$ within the acoustic domain as

$$\psi(\mathbf{x}_0)=h(p(\mathbf{x}_0),\mathbf{u}) \tag{22}$$

where the function $h(p,\mathbf{u})$ is assumed to be continuously differentiable with respect to its arguments. The variation of the performance measure with respect to the design variable becomes

$$\psi'=\frac{d}{d\tau}[h(p(\mathbf{x};\mathbf{u}+\tau\delta\mathbf{u}),\mathbf{u}+\tau\delta\mathbf{u})]\bigg|_{\tau=0}=h_{,p}p'+h_{,\mathbf{u}}^T\delta\mathbf{u} \tag{23}$$

where $h_{,p}=\partial h/\partial p$ and $h_{,\mathbf{u}}=\partial h/\partial\mathbf{u}$ can be obtained from the definition of the function h. Thus, from the solution to the acoustic design sensitivity Eq. (19), the sensitivity of ψ can readily be calculated. However, the calculation of p' also requires the solution to the structural sensitivity Eq. (18).

3.2 Adjoint Variable Method. Since the number of design variables is larger than the number of active constraints in many optimization problems, the adjoint variable method is attractive. Although the adjoint variable method is known to be limited to a symmetric operator problem, in this section, it is further extended to non-symmetric complex operator problems. Since the adjoint variable method is directly related to the performance measure, the structural and acoustic performance measures are treated separately. In case of the acoustic performance measure, a sequential adjoint variable method is introduced.

The acoustic performance measure ψ in Eq. (22) is defined at point $\mathbf{x}_0$, and its sensitivity expression in Eq. (23) contains p', which has to be explicitly expressed in terms of $\delta\mathbf{u}$. The objective is to express p' in terms of $\mathbf{v}'$ such that an adjoint problem can be defined. By substituting the relation in Eq. (19) into the sensitivity expression of Eq. (23), and by using the relation in Eq. (13), we obtain

$$\psi'=h_{,\mathbf{u}}^T\delta\mathbf{u}+h_{,p}p'=h_{,\mathbf{u}}^T\delta\mathbf{u}+h_{,p}[b(\mathbf{x}_0;\mathbf{v}')+e(\mathbf{x}_0;A^{-1}\circ B(\mathbf{v}'))] \tag{24}$$

In Eq. (24), $\alpha=1$ is used since $\mathbf{x}_0$ is the interior point. Thus, ψ' is expressed in terms of $\mathbf{v}'$. The second term on the right side of the above equation can be used to define the adjoint load by substituting $\boldsymbol{\lambda}$ for $\mathbf{v}'$. Hence, the following form of the adjoint problem is obtained:

$$j\omega d_u(\overline{\boldsymbol{\lambda}},\boldsymbol{\lambda})+\kappa a_u(\overline{\boldsymbol{\lambda}},\boldsymbol{\lambda})=h_{,p}[b(\mathbf{x}_0;\overline{\boldsymbol{\lambda}})+e(\mathbf{x}_0;A^{-1}\circ B(\overline{\boldsymbol{\lambda}}))],\quad \forall\,\overline{\boldsymbol{\lambda}}\in Z \tag{25}$$

where an adjoint solution $\boldsymbol{\lambda}^*$ is desired. After calculating $\boldsymbol{\lambda}^*$, the sensitivity of ψ can be obtained using Eq. (18), as

$$\psi'=h_{,\mathbf{u}}\delta\mathbf{u}+\ell'_{\delta\mathbf{u}}(\boldsymbol{\lambda})-j\omega d'_{\delta\mathbf{u}}(\mathbf{v},\boldsymbol{\lambda})-\kappa a'_{\delta\mathbf{u}}(\mathbf{v},\boldsymbol{\lambda}) \tag{26}$$

It is interesting to note that even if ψ is a function of pressure p, its sensitivity expression in Eq. (26) does not require the value of p; only the structural solution $\mathbf{v}$ and the adjoint solution $\boldsymbol{\lambda}^*$ are required in the calculation of ψ'.

Consider a discrete form of the adjoint load. Equation (25) can be written in the discrete system as

$$[j\omega\mathbf{M}+\kappa\mathbf{K}]\{\boldsymbol{\lambda}^*\}=h_{,p}[\{\mathbf{b}\}+[\mathbf{B}]^T[\mathbf{A}]^{-T}\{\mathbf{e}\}] \tag{27}$$

where the right side corresponds to the adjoint load in the discrete system. If $h=p(\mathbf{x}_0)$, the pressure at a point $\mathbf{x}_0$, then $h_{,p}$ in Eq. (27) will represent Dirac-Delta measure, which corresponds to a point load. Instead of computing the inverse matrix, let us define an acoustic adjoint problem in BEA as

$$[\mathbf{A}]^T\{\boldsymbol{\eta}\}=\{\mathbf{e}\} \tag{28}$$

where the acoustic adjoint solution $\{\boldsymbol{\eta}\}$ is desired. Even though the coefficient matrix $[\mathbf{A}]$ is not symmetric, the adjoint Eq. (28) can still use the factorized matrix of the BEA Eq. (12). By substituting $\{\boldsymbol{\eta}\}$ into Eq. (27), we obtain the structural adjoint problem as

$$[j\omega\mathbf{M}+\kappa\mathbf{K}]\{\boldsymbol{\lambda}^*\}=h_{,p}[\{\mathbf{b}\}+[\mathbf{B}]^T\{\boldsymbol{\eta}\}] \tag{29}$$

Note that the acoustic adjoint solution $\{\boldsymbol{\eta}\}$, which is obtained from BEA, is required to compute the structural adjoint load, and then frequency response re-analysis provides the structural adjoint solution $\{\boldsymbol{\lambda}^*\}$. Thus, two different adjoint problems are defined: the first is similar to BEA, and is used to compute the adjoint load, while the second is similar to the structural frequency-response FEA.

3.3 Numerical Method. The variational equation of the harmonic motion of a continuum model, Eq. (9), can be reduced to a set of linear algebraic equations by discretizing the model into elements using FEA. It is assumed that the structural finite element and the acoustic boundary element meshes match at their interfaces. The acoustic pressure $p(\mathbf{x})$ and structural velocity $\mathbf{v}(\mathbf{x})$ are approximated using shape functions and nodal variables for each element in the discretized model as

$$\left.\begin{aligned}\mathbf{v}(\mathbf{x})&=\mathbf{N}_s(\mathbf{x})\mathbf{v}^e\\ p(\mathbf{x})&=\mathbf{N}_a(\mathbf{x})\mathbf{p}^e\end{aligned}\right\} \tag{30}$$

where $N_s(\mathbf{x})$ and $N_a(\mathbf{x})$ are matrices of shape functions for the velocity and pressure, respectively, and $\mathbf{v}^e$ and $\mathbf{p}^e$ are the element nodal variable vectors. Substituting Eq. (30) into Eq. (9) and carrying out integration yields the same matrix equation as Eq. (10), rewritten here

$$[j\omega\mathbf{M}+\kappa\mathbf{K}]\{\mathbf{v}(\omega)\}=\{\mathbf{f}(\omega)\} \tag{31}$$

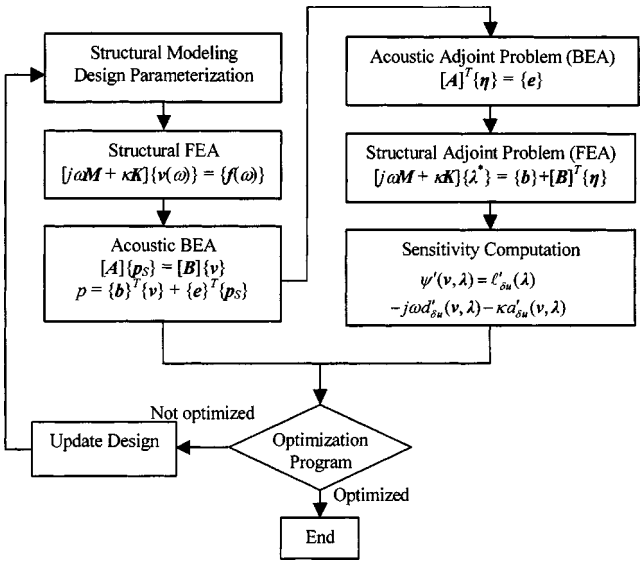

Fig. 1 Computational procedure of FEA-BEA optimization

After obtaining the structural velocity, BEA is used to evaluate the pressure response on the boundary, as well as within the acoustic domain, as described in Section 2.2.

Figure 1 shows the computational procedure for the adjoint variable method with a structural FEA and an acoustic BEA code. Even though FEA and BEA are used to evaluate the acoustic performance measure, only the structural response **v** is required to perform DSA. The adjoint load is calculated from the transposed BEA, and the adjoint equations are then numerically solved using the FEA code with the same finite element model used for the original structural analysis. Numerical solutions are used to compute the design sensitivity, and the integration of the design sensitivity expressions in Eq. (26) can be evaluated using a numerical integration method, such as the Gauss quadrature method [1]. The integrands are functions of the state variable, the adjoint variable, and gradients of both variables.

4 Design Optimization

For structural-acoustic problem, the sequential FEA-BEA analysis calculates the performance measure (noise and vibration), and the adjoint variable method for DSA calculates the sensitivity of the performance measure. This information is utilized by the optimization program to search for the optimum design.

4.1 Optimization Procedure for a Sequential Structural-Acoustic Problem. The gradient-based optimization algorithms are commonly used in engineering design and optimization. The performance measure and its sensitivity are required for the gradient-based optimization process. Figure 1 shows the computational procedure for the optimization of the sequential structural-acoustic problem using a gradient-based optimization algorithm. Once the design variable, cost function, and design constraints are defined, the proposed sequential FEA-BEA and reverse adjoint variable DSA method are employed to compute the performance measure and their sensitivity, which will be input to the optimization program to search for the optimum design. The process will loop until an optimum design is achieved.

4.2 Numerical Example—NVH Optimization of a Complex Vehicle Structure. One of important applications of the proposed method is structure-borne noise reduction of a vehicle. Figure 2 shows finite element and boundary element models of a next generation hydraulic hybrid vehicle [19]. In addition to the powertrain vibration and wheel/terrain interaction, the hydraulic pump is a source of vibration, considered as a harmonic excitation. Because of this additional source of excitation, vibration and noise is more significant than with a conventional powertrain. The object of the design optimization is to minimize the vehicle weight as well as maintaining noise and vibration at the driver's ear position to the desirable levels.

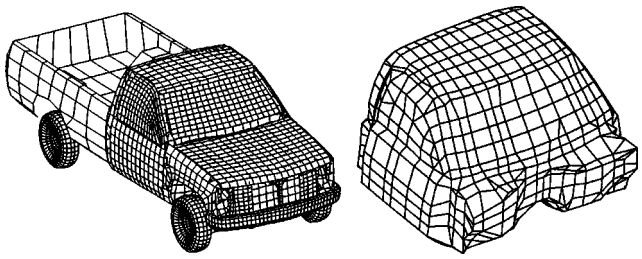

Fig. 2 Vehicle structure FE model and acoustic BE model of the cabin part

From the powertrain analysis and rigid body dynamic analysis, the harmonic excitations at twelve locations are obtained. Frequency response analysis is carried out on the structural FE model using MSC/NASTRAN to obtain the velocity response, corresponding to the frequency range up to 100 Hz. COMET/ACOUSTICS [9] is employed to obtain the acoustic pressure performance measure in the acoustic domain as shown in Fig. 2. Once the acoustic performance measure and sensitivity information are obtained according to the procedure illustrated in Fig. 1, the sequential quadratic programming algorithm in DOT (Design Optimization Tool) [22] is used to search for the optimum design.

4.2.1 FEA-BEA NVH Analysis and Adjoint Design Sensitivity Analysis of the Vehicle. The sequential FEA-BEA analysis is performed on the vehicle model. In this example, the noise level at the passenger compartment is chosen as the performance measure, and vehicle panel thicknesses are chosen as design variables. The sound pressure level frequency response up to 100 Hz at the driver's ear position is obtained and illustrated in Fig. 3 and the numerical results at selected frequencies are shown in Table 1.

The highest sound pressure level occurs at 93.6 Hz, which is the first acoustic resonant mode under 100 Hz. Figure 4 shows the sound pressure level distribution inside the cabin compartment at this frequency. The sound pressure level at the driver's ear position is 77.78 dB. Design modification is carried out mainly focusing on reducing the peak noise level in the neighborhood of this frequency.

The vehicle structure is divided into forty different panels, whose thicknesses are selected as design variables in this ex-

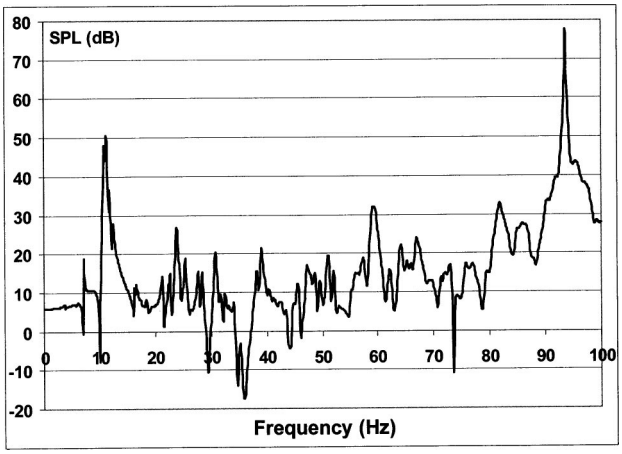

Fig. 3 Sound pressure level (SPL) frequency response at driver's ear position (at initial design)

Table 1 Sound pressure levels at driver's ear position at selected frequencies

Frequency (Hz)	Pressure (kg/mm·sec^2)	Phase Angle (degree)
7.1	0.78747$E-04$	247.53
10.8	0.22699$E-02$	211.33
11.2	0.31111$E-02$	129.66
23.7	0.20014$E-03$	282.12
30.7	0.95681$E-04$	271.96
39.0	0.10764$E-03$	253.43
47.3	0.64318$E-04$	66.916
57.4	0.79145$E-04$	101.45
59.2	0.36350$E-03$	16.567
67.0	0.14299$E-03$	226.53
81.8	0.41087$E-03$	264.22
93.6	0.71486$E-01$	64.267

ample. In order to carry out DSA, the acoustic adjoint problem in Eq. (28) and the structural adjoint problem in Eq. (29) are solved to obtain the adjoint response $\boldsymbol{\lambda}^*$. Using the original velocity response $\mathbf{v}$ and the adjoint response $\boldsymbol{\lambda}^*$, the numerical integration of Eq. (26) is carried out to calculate the sensitivity for each structural panel, as shown in Table 2. The sensitivity contributions from all panels are normalized in order to compare the relative magnitude of the design sensitivity. The results indicate that a thickness change in the chassis component has the greatest potential for achieving reduction in the sound pressure level. Since the numerical integration process is carried out on each finite element, the element sensitivity information can be obtained without any additional effort. Figure 5 plots the sensitivity contribution from each element to the sound pressure level. Such graphic-based sensitivity information is very helpful for the design engineer to determine a desirable direction of design modification.

4.2.2 Optimization of the Vehicle Model. The design optimization problem is to search a design with minimum weight, while the noise level at the driver's ear position can be controlled to a desirable level. The weight (mass) of the vehicle is chosen as the objective function and the sound pressure level at the driver's ear position is chosen as a design constraint. The sound pressure level of 65.0 dB, which is 12.78 db less than the maximum sound pressure level (SPL) at the initial design and equivalent to more than 75% noise reduction, is used as design constraints.

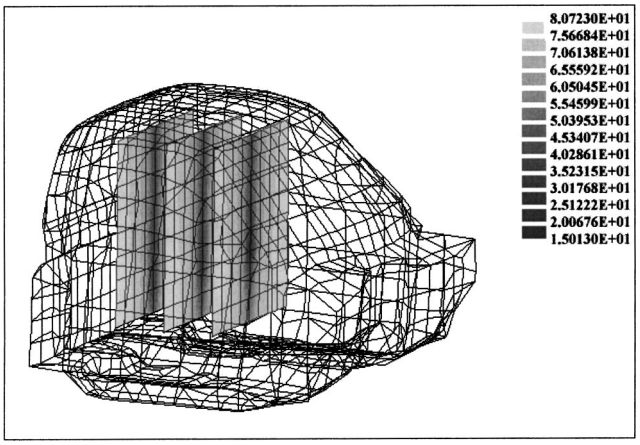

Fig. 4 Sound pressure plot at 93.6 Hz: 77.78 dB at driver's ear position (at initial design)

Table 2 Normalized sound pressure sensitivity w.r.t. panel thickness

Component	Sensitivity	Component	Sensitivity
Chassis	−1.0	Chassis MTG	−0.11
Left wheelhouse	−0.82	Chassis connectors	−0.10
Right door	0.73	Right fender	−0.07
Cabin	−0.35	Left door	−0.06
Right wheelhouse	−0.25	Bumper	−0.03
Bed	−0.19	Rear glass	0.03

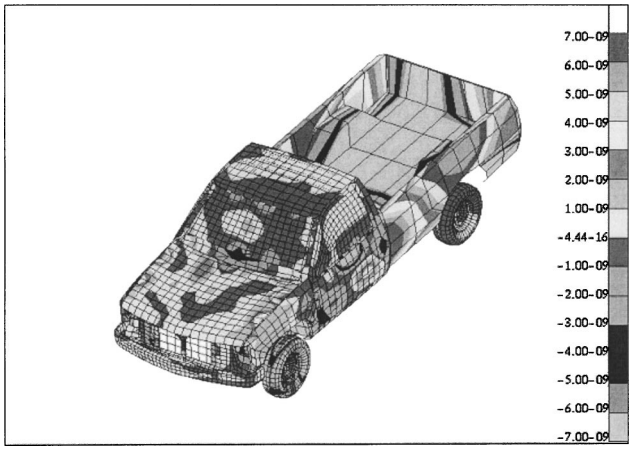

Fig. 5 Element design sensitivity plot w.r.t. panel thickness

Although, the maximum sound pressure occurs at 93.6 Hz at the initial design, the frequency where the maximum pressure occurs may shift during design process. However, it is difficult to constrain all continuous frequency ranges. Thus, a fixed set of discrete frequencies is chosen in order to evaluate the sound pressure level. Since the most significant acoustic resonance occurs around 93.6 Hz, a total of eleven equally distributed frequencies in the neighborhood of 93.6 Hz are chosen to evaluate the sound pressure level during design optimization.

Among the forty design variables that are used to calculate the design sensitivity information, ten design variables are selected to change during design optimization because some of panel thicknesses are difficult to change for design purposes and some of them are related to the vehicle's dynamic performance. Ten selected design variables are panel thicknesses of Chassis, Fender-Left, Fender-Right, Wheelhouse-Left, Wheelhouse-Right, Cabin, Door-Left, Door-Right, Chassis-Conn, and Chassis-MTG, which significantly contribute to the sound and vibration level inside the cabin. The design space is chosen such that each design variable can change up to ±50%. Accordingly, the design optimization problem is formulated as

Minimize Cost Function $c(\mathbf{u})$=mass

Subject to Design Constraints

$$g_i = p(\mathbf{u}, f_i) - 65.0 \leqslant 0,\ i = 1, \ldots, 11$$

$$0.5\ \ \mathbf{u}_0 \leqslant \mathbf{u} \leqslant 1.5\mathbf{u}_0$$

$$f_i = (93.2 + i \times 0.1)\ \ \text{Hz}$$

Design Variables: $\mathbf{u} = [h_1, h_2, \ldots, h_{10}]^T$

Table 3 Optimum design result

Design Variable	Initial Design	Optimum Design
x_1 (Chassis)	3.137	1.568500
x_2 (Fender-Left)	0.800	0.400200
x_3 (Fender-Right)	0.800	0.400200
x_4 (Wheelhouse-Left)	0.696	0.348000
x_5 (Wheelhouse-Right)	0.696	0.368218
x_6 (Cabin)	2.500	1.250080
x_7 (Door-Left)	1.240	1.859970
x_8 (Door-Right)	1.240	0.620000
x_9 (Chassis-Conn)	3.611	1.805500
x_{10} (Chassis-MTG)	3.000	1.500000

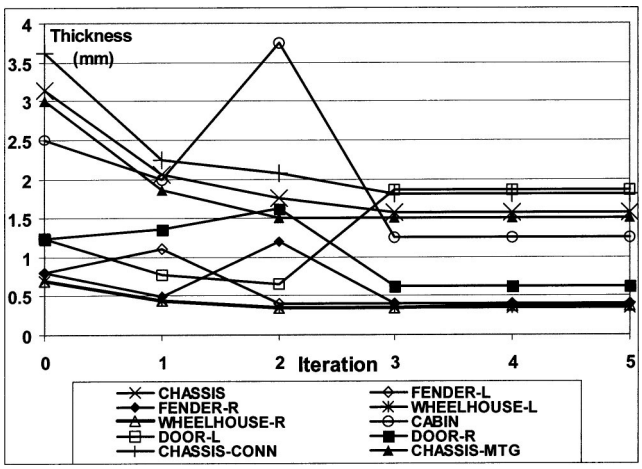

Fig. 6 Design variable history

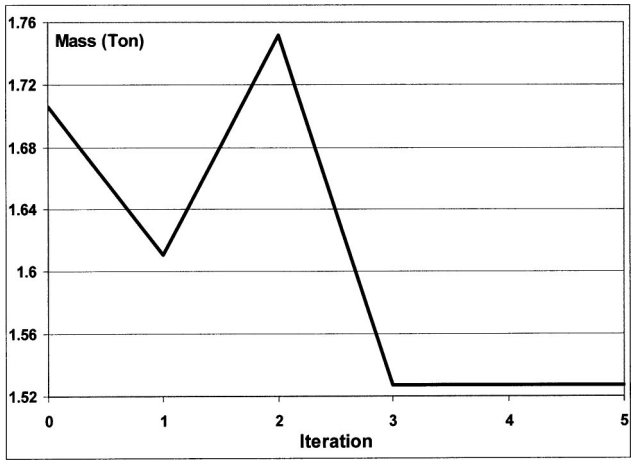

Fig. 7 Cost function history

The design optimization procedure illustrated in Fig. 1 is carried out. A seamless integration between FEA, BEA, sensitivity module, and optimization module is critical in an automated design process. MSC/NASTRAN is used for frequency response FEA, while COMET/ACOUSTICS is used for the acoustic BEA. The design sensitivity information is calculated from the Design Sensitivity Analysis and Optimization (DSO) Tool [21]. A sequential quadratic programming algorithm in DOT is used for design optimization. The optimization problem is converged after five design iterations. A total of 15 response analyses and five design sensitivity analyses have been performed during design optimization. Table 3 compares the design variables between the initial and optimum designs.

Figure 6 illustrates the design variable history during optimization. It is observed that all the design variables are decreased to reach the lower bound except one of them, the left door, which increased to the upper limit. Table 4 and Fig. 7 show the history of the cost function. The total mass of the vehicle is reduced from 1705.834 Kg to 1527.182 Kg, which is 178.652 Kg reducing, while the design constraints are satisfied. Figure 8 shows the sound pressure distribution inside the cabin before and after optimization.

Figure 9 plots the change of the sound pressure level at the driver's ear position for the frequency range from 93.3 to 94.3 Hz during the optimization process. At the optimum design, the peak noise level is reduced to 65.0 dB, a total amount of 12.78 dB reduction. Note that the frequency, at which the maximum sound pressure appears, is shifted from 93.6 Hz to 93.7 Hz. However, this is not due to the shift of the acoustic resonant mode. The acoustic resonant mode still remains unchanged because of the same geometry of the acoustic space. This indicates that the correct acoustic resonant frequency should be in-between 93.6 and 93.7 Hz. However, the selected design constraints are broad enough to cover the frequency range where the maximum noise level would occur.

Table 4 History of cost function and design constraints

History	Cost Function (Mass, ton)	Design Constraint g_4 (dB) at $f=93.6$ Hz	Design Constraint g_5 (dB) at $f=93.7$ Hz
Initial Design	1.705834	77.780	76.318
Iteration 1	1.610563	80.473	77.825
Iteration 2	1.751358	71.247	69.662
Iteration 3	1.527082	66.185	67.307
Iteration 4	1.527182	62.586	65.000
Iteration 5 (Optimum)	1.527182	62.586	65.000

However, since the selected design constraints do not cover the entire frequency range, concern may arise that, while the peak noise level around 93.6 Hz is reduced, some other undesirable noises may occur at other frequencies. In order to check, the sound pressure levels at all frequencies below 100 Hz at the optimum design are computed and compared with initial design as plotted in Fig. 10. The result indicates that the noise level at all frequency range is maintained under the constraint value. Al-

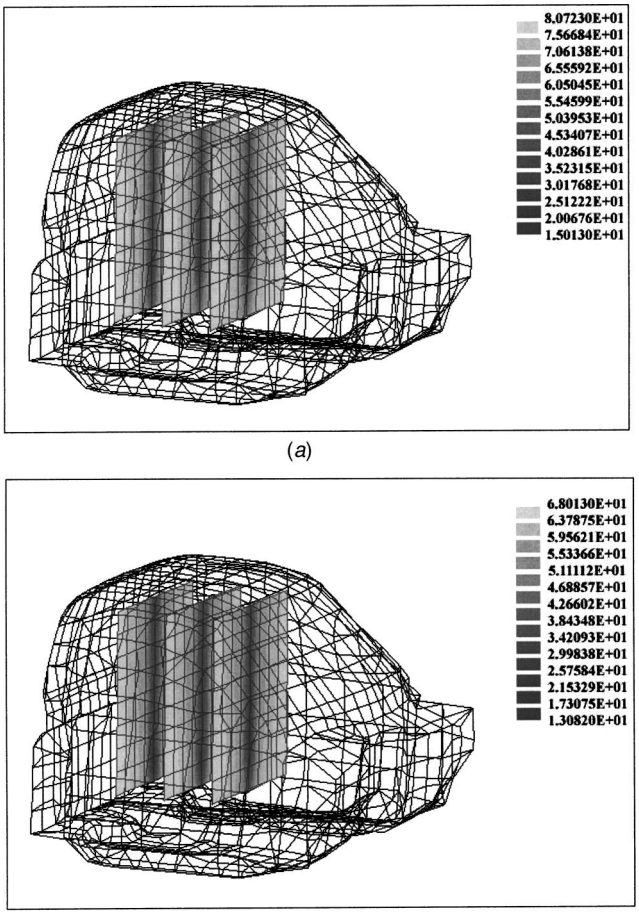

Fig. 8 Acoustic pressure distribution inside cabin (initial design at 93.6 Hz and optimum design at 93.7 Hz)

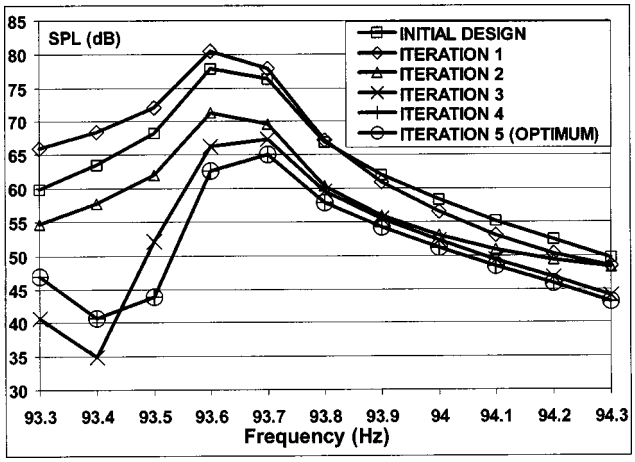

Fig. 9 Design constraints history in the frequency range between 93.3 and 94.3 Hz

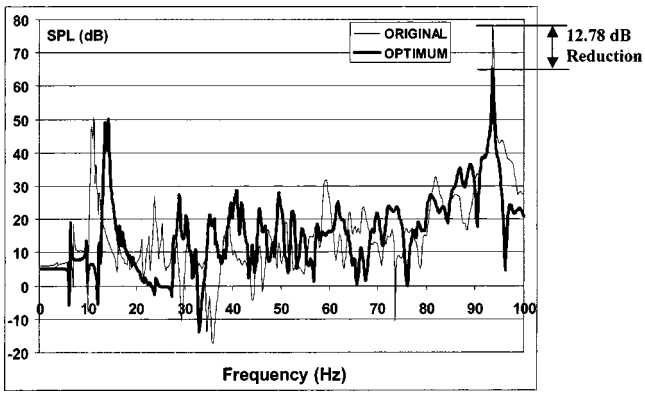

Fig. 10 Sound pressure level frequency response at driver's ear position (initial design and optimum design)

though the sound pressure levels at some other frequencies increased, the value is still within the constraint limit. On the other hand, proper selection of constraints is effective and computationally efficient.

5 Conclusions

Under the assumption that acoustic behavior does not influence structural behavior, design sensitivity analysis and optimization of a sequential structural-acoustic problem is presented using FEA-BEA. In the adjoint variable method, a reverse sequential adjoint problem is formulated, in which the adjoint load is calculated by solving a boundary adjoint problem and the adjoint solution is calculated from a structural adjoint problem. Design optimization based on the sequential FEA-BEA analysis and reverse adjoint variable DSA method is carried out on a concept vehicle structure with satisfactory results, by reducing the noise level at the driver's ear position significantly while lowering the weight considerably.

Acknowledgments

This research is supported by the Automotive Research Center that is sponsored by the US Army TARDEC under Contract DAAE07-94-C-R094. The authors sincerely appreciate Profs. C. Pierre and N. Vlahopoulos, and Drs. Z.-D. Ma and M. Castanier for their truck model and collaboration in ARC research.

References

[1] Hughes, T. J. R., 1987, *The Finite Element Method*, Prentice-Hall, Englewood Cliffs, NJ.
[2] Kythe, P. K., 1995, *Introduction to Boundary Element Methods*, CRS Press, Florida.
[3] Lyon, R., 1975, *Statistical Energy Analysis of Dynamical Systems: Theory and Application*, The MIT Press, Cambridge, MA.
[4] Rybak, S. A., 1972, "Waves in Plate Containing Random Inhomogeneities," Sov. Phys. Acoust., **17**(3), pp. 345–349.
[5] Nefske, D. J., and Sung, S. H., 1989, "Power Flow Finite-Element Analysis of Dynamic-Systems—Basic Theory and Application to Beams," ASME J. Vibr., Acoust., Stress, Reliab. Des., **111**(1), pp. 94–100.
[6] Bernhard, R. J., and Huff, J. E., 1999, "Structural-Acoustic Design at High Frequency Using the Energy Finite Element Method," ASME J. Vibr. Acoust., **121**(3), pp. 295–301.
[7] Vlahopoulos, N., Garza-Rios, L. O., and Mollo, C., 1999, "Numerical Implementation, Validation, and Marine Applications of an Energy Finite Element Formulation," J. Ship Res., **43**(3), pp. 143–156.
[8] Gockel, M. A., 1983, *MSC/NASTRAN Handbook for Dynamic Analysis*, The MacNeal-Schwendler Corporation, 815 Colorado Blvd., Los Angeles, CA.
[9] *COMET/ACOUSTICS User's Manual*, Automated Analysis Corporation.
[10] Ma, Z.-D., and Hagiwara, I., 1991, "Sensitivity Analysis-Method for Coupled Acoustic-Structural Systems Part 2: Direct Frequency-Response and Its Sensitivities," AIAA J., **29**, pp. 1796–1801.
[11] Choi, K. K., Shim, I., and Wang, S., 1997, "Design Sensitivity Analysis of Structure-Induced Noise and Vibration," ASME J. Vibr. Acoust., **119**, pp. 173–179.
[12] Nefske, D. J., Wolf, J. A., and Howell, L. J., 1982, "Structural-Acoustic Finite Element Analysis of the Automobile Passenger Compartment: A Review of Current Practice," J. Sound Vib., **80**, pp. 247–266.
[13] Salagame, R. R., Belegundu, A. D., and Koopman, G. H., 1995, "Analytical Sensitivity of Acoustic Power Radiated From Plates," ASME J. Vibr. Acoust., **117**, pp. 43–48.
[14] Scarpa, F., 2000, "Parametric Sensitivity Analysis of Coupled Acoustic-Structural Systems," ASME J. Vibr. Acoust., **122**, pp. 109–115.
[15] Smith, D. C., and Bernhard, R. J., 1992, "Computation of Acoustic Shape Design Sensitivity Using a Boundary Element Method," ASME J. Vibr. Acoust., **114**, pp. 127–132.
[16] Cunefare, K. A., and Koopman, G. H., 1992, "Acoustic Design Sensitivity for Structural Radiators," ASME J. Vibr. Acoust., **114**, pp. 179–186.
[17] Kane, J. H., Mao, S., and Everstine, G. C., 1991, "Boundary Element Formulation for Acoustic Shape Sensitivity Analysis," J. Acoust. Soc. Am., **90**, pp. 561–573.
[18] Matsumoto, T., Tanaka, M., and Yamada, Y., 1995, "Design Sensitivity Analysis of Steady-State Acoustic Problems Using Boundary Integral Equation Formulation," JSME Int. J., Ser. C, **38**, pp. 9–16.
[19] Kim, N. H., Dong, J., Choi, K. K., Vlahopoulos, N., Ma, Z.-D., Castanier, M. P., and Pierre, C., 2003, "Design Sensitivity Analysis for Sequential Structural-Acoustic Problems," J. Sound Vib., **263**(3), June, pp. 569–591.
[20] Kim, N. H., Choi, K. K., Dong, J., Pierre, C., Vlahopoulos, N., Ma, Z.-D., and Castanier, M., 2001, "A Sequential Adjoint Variable Method in Design Sensitivity Analysis of NVH Problems," *ASME International Mechanical Engineering Congress and Exposition (IMECE'01)*, November 11–16, New York, NY.
[21] Chang, K. H., Choi, K. K., Tsai, C. S., Chen, C. J., Choi, B. S., and Yu, X., 1995, "Design Sensitivity Analysis and Optimization Tool (DSO) for Shape Design Applications," Computing Systems in Engineering, **6**(2), pp. 151–175.
[22] Vanderplaats, G. N., 1997, *DOT User's Manual*, VMA Corp., Colorado Springs, CO.
[23] Horvath, J., 1966, *Topological Vector Spaces and Distributions*, Addison-Wesley, London.
[24] Dimarogonas, A. D., 1976, *Vibration Engineering*, West Publishing Co., St. Paul, MN.